Robust empirical correlation development for subcooled flow boiling heat transfer in internal combustion engines

Ali Qasemian, Ali Keshavarz

Abstract— The subjects of heat transfer and cooling system are very important topics in the Internal Combustion Engines (ICE). In modern cooling systems, low weight, small size and high compactness are the critical designing criteria that requires heat transfer enhancement. Using the boiling phenomenon is one of the methods to increase heat transfer in the coolant system of an ICE. Due to the importance of this phenomenon, the accuracy of the existing model must be improved continuously. The Boiling which takes place in some of the cooling water jacket can be analyzed with the combination of forced convection and pool boiling models. A suppression factor is multiplied with the pool boiling model to lower its impact. In this study, a new robust empirical correlation is developed mathematically along with existing models. To ensure the accuracy of this new proposed correlation, an experimental test rig was set up and comprehensive data was collected. It showed good consistency between the new developed model and the experimental data. This correlation will predict the flow boiling in the ICE cooling passages better than previous models.

Index Terms— Flow boiling, Heat transfer, Internal combustion engine

1 INTRODUCTION

The heat released in a combustion chamber of an engine is divided into three main parts. Only about one third of the input energy is converted to useful output power and the rest is wasted by means of exhaust gases and cooling system. The main goal of the cooling system is to keep the engine components at proper temperature. Although the heat rejected to the coolant of an ICE varied with the type, load and speed of an engine, but in general, it is about 17 to 26 percent of the input energy in a SI engine and 16 to 35 percent in a CI engine [1].
Some regions of the cylinder head such as exhaust valve and valves bridges may experience heat fluxes as high as 10 MW/m^2 during the combustion period [1]. This high heat flux in one hand and the industry demand for lower cooling system power and downsizing the engine in the other hand requires cooling system enhancement. Clough [2] proposed precision cooling system due to different heat fluxes regions along the water jacket. In the precision cooling the heat transfer coefficient is increased around high heat flux regions to achieve uniform temperature. In a water cooled engine, the heat is removed by forced convection through the water jacket. Therefore to increase the heat rejection from the chamber walls, the convection coefficient should be somehow enhanced. A method which causes a considerable increase in convection coefficient is boiling phenomenon [3, 4]. This motivates the researchers to study the nature and modeling of this phenomenon in ICE.
Boiling takes place at a solid-liquid interface in which the temperature of the solid surface is higher than saturation temperature of the liquid as shown in figure 1. When the fluid adjacent to the hot surface, has no motion, the process called pool boiling and otherwise it called flow boiling. It also can be classified as saturated boiling and subcooled boiling. In the saturated boiling regime, the bulk temperature of the fluid is at the saturation temperature of it and in the subcooled boiling regime the bulk temperature of the fluid is less than its saturation temperature. The boiling phenomenon which may occur in some regions of an ICE water jacket is a subcooled flow boiling regime. During the boiling phenomenon, due to the latent heat of the fluid, huge amount of energy is transferred from the hot solid surface. By increasing the wall temperature, the rate and number of bubbles creation increases and consequently the heat transfer coefficient increases. At a specific point of the wall temperature- called CHF[1]- the velocity of bubble formation outpaces the velocity of the bubbles departure from the heated surface. In this stage, gradually a vapor layer covers the heated surface and the heat transfer coefficient decreases which must be avoided in the ICE cooling.
Finlay [5] is one of the pioneers in the modeling of subcooled flow boiling in ICE. He simulated the boiling process in the water jacket experimentally and theoretically. Mixture of water and ethylene glycol is used as the coolant. Finlay showed that in high flow velocities, the forced convection is dominating mode of the heat transfer. Whereas, at low flow velocities strong nucleate boiling takes place. He used the Chen's correlation [6] as theoretical model and reported good agreement between this and the experimental results. Chen suggests by equation 1 the heat flux removal by the flow boiling can be considered by two parts namely forced convection and pool boiling term multiplies by a suppression factor.

$$q''_{w,fb} = q''_{fc} + q''_{nb} \times S_{Chen} = h_{fc}\left(T_w - T_f\right) + h_{nb}\left(T_w - T_s\right) \times S_{Chen} \quad (1)$$

Chen used Dittus-Boelter [7] and Forster-Zuber [8] correlation for force convection and boiling HTC respectively. The effect of surface roughness was not considered in either of them. The

- *Ali Qasemian, Ph. D. Student, K. N. Toosi University of Technology, Tehran, Iran, 0982184063241, aghasemian@dena.kntu.ac.ir*
- *Ali keshavarz, Associate Professor, K. N. Toosi University of Technology, Tehran, Iran, 0982184063241, Keshavarz@kntu.ac.ir*

[1] Critical heat flux

effect of surface roughness on boiling phenomenon was studied experimentally by Campbell et al [9]. Robinson et al [10, 11] continued Campbell work theoretically. Although they used Chen's model like Finlay, but they modify the force convection HTC. Robinson's simulation is more precise than Finlay results. At high flow velocity that force convection dominates, there is a good agreement between the experimental and Robinson's model. But at low flow velocity that the boiling plays an important role some deviations appear between the simulation and experimental results. The subcooled flow boiling was investigated experimentally and theoretically by Steiner [12]. A new suppression factor called BDL is used in Chen's model. Due to this modification a good consistency is reported between Steiner's result and the experimental data. Another experimental and theoretical research was conducted on an ICE by Lee et al [13,14] based on Chen's model. Based on the experimental results Lee introduced a factor of 2 should be multiplied by the forced convection term.

Despite all the efforts done by researchers, lack of close consistency between the experimental data and proposed models especially in low velocity that boiling has a considerable role in heat transfer is seen. The purpose of this study is to improve the accuracy of the flow boiling heat transfer modeling.

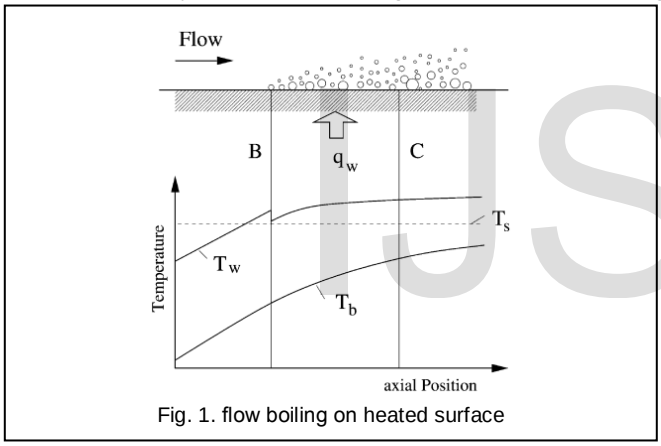

Fig. 1. flow boiling on heated surface

2 MATHEMATICAL FORMULATION OF THE SUBCOOLED fIOW BOILING

Many correlations have been proposed in order to model the flow boiling. Most of these correlations as shown in eq. (1), are based on this principle that the boiling heat flux consists of two components: force convection and pool boiling. This concept of additive contributions was introduced by Rohsenow [15] firstly. Although he proposed it for saturated flow boiling, but it is being also used for subcooled flow boiling specially in ICE water jacket [5, 9-14]. To model the flow boiling, a coefficient called suppression factor should multiply by nucleate pool boiling heat flux to undermine the severity of the boiling effect.

2.1 Convection Term

The general correlation for the convection term is given as follows

$$q''_{fc} = h_{fc}(T_w - T_b) \tag{2}$$

Many correlations were introduced for HTC. The most popular ones are those introduced by Dittus-Boelter and Gnielinski [3]. These are given in equations 3 and 4 respectively.

$$Nu_{Dittus\text{-}Boelter} = \frac{h_{fc}D_h}{k} = 0.023Re^{0.8}Pr^{0.4} \tag{3}$$

$$Nu_{Gnielinski} = \frac{h_{fc}D_h}{k} = \frac{Re_D Pr\left(\frac{f}{8}\right)}{1.07 + \left(12.7\left(\frac{f}{8}\right)^{\frac{1}{2}}\right)\left(Pr^{\frac{2}{3}} - 1\right)} \tag{4}$$

These correlations are given for hydraulically and thermally fully developed conditions. Considering the effect of surface roughness is the main advantage of the Gnielinski correlation to the Dittus-Boelter one. For rough pipes, the friction factor can be read from a standard Moody diagram, which defines the friction factor as a function of Reynolds number and relative roughness. Alternatively, several correlations are available for predicting the friction factor as a function of relative roughness and Reynolds number. One of the most widely accepted correlation for friction factor is as follows [16]:

$$f = \frac{0.25}{\left(\log\frac{e}{3.7D_h} + \frac{5.74}{Re^{0.9}}\right)^2} \tag{5}$$

To simulate the boiling phenomenon in the water jacket of an ICE, the experimental setup is designed in such way that has more resemblance to the water jacket of a cylinder head. In this study, the experimental data of three different setups are used for the validation. Where it is needed, the effect of entrance length and the unheated length [17] must be included in the calculations. Furthermore due to the large fluid viscosity variation near the hot surface, the Seider-Tate [3] correction factor should be applied. Hence, the final Gnielinski HTC which includes the three above corrections can be stated as eq. (6).

$$h_{fc} = h_{fc,Gnielinski} \times \left(\frac{\mu_b}{\mu_w}\right)^{0.14} \times \left(1 + 23.99Re^{-0.23}\left(\frac{x}{D_h}\right)^{0.7}\right) \times \left(\frac{1}{\left(1 - \left(\frac{x_0}{x}\right)^{0.9}\right)^{\frac{1}{9}}}\right) \tag{6}$$

2.2 Boiling Term

The heat flux due to the pool nucleate boiling on a hot surface is given by the following equation.

$$q''_{nb} = h_{nb}(T_w - T_s) \tag{7}$$

Many researchers have studied the boiling phenomenon experimentally and introduced some correlations for its simulation. Rohsenow [18] presented eq. (8) for calculating the nucleate boiling heat transfer coefficient. This is among the oldest and most widely used one.

$$h_{nb,Rohsenow} = \left[\left(\frac{C_P}{C_{sf}\mu_l h_{lg}}\right)\left(\frac{T_w - T_s}{}\right)\cdot\left(\frac{k\ \Delta\rho}{\sigma}\right)\right]^{\frac{1}{n}}\left(\ f\ \lg\sqrt{\frac{g}{}}\right) \tag{8}$$

Where n = 0.33, m = 0 for water and m = 0.7 for other fluids. The recommended values of parameter C_{sf} for various solid–fluid combination are given in Rohsenow [19]. This parameter varies in the relatively wide range $0.003 < C_{sf} < 0.0154$. A value of 0.013 is recommended for unknown pairs.

The other widely used correlation for hnb is Forster-Zuber's

[8] model given as eq.(9). Although the Forster-Zuber's model is simple and general but it doesn't consider the surface roughness.

$$h_{nb,Forster-Zuber} = 0.00122\left[\frac{k_l^{0.79}\rho C_{p,l}^{0.45}{}_{l}^{0.49}}{\sigma^{0.5}\mu_l^{0.29}(h\rho)_{lg}^{0.24}}\right]\times(\Delta T_s)^{0.24}(\Delta p_s)^{0.75} \quad (9)$$

In another experimentally work, Cooper [20] derived correlation that is applicable to different fluids.

$$h_{nb,Cooper} = \left[55.0\left(\frac{p}{p_{cr}}\right)^{n_1}\left(-\log_{10}\frac{p}{p_{cr}}\right)^{-0.55}M^{-0.5}\right]^3\times(T_w - T_s)^2 \quad (10)$$

In the above equation, the parameter "n_1" is given by eq. (11)

$$n_1 = 0.12 - 0.21\log_{10}R_p \quad (11)$$

Equation (12) is another correlation based on extensive experimental data which was given by Gorenflo [4].

$$h_{Gorenflo} = \left[\frac{q_0''^{n}}{h_0 F_{PR}\left(\frac{R_p}{R_{p_0}}\right)^{0.133}(T_w - T_{sat})^{n_2}}\right]^{\frac{1}{n_2-1}} \quad (12)$$

In the above equation $q_0'' = 20000\ W/m^2$ and "h_0" is the heat transfer coefficient corresponding to q_0'' at the reference reduced pressure P_{r0}=0.1. The reference surface roughness parameter is R_{P0}=0.4μm. The values of h0 and pcr for a number of fluids are given in references [21, 22]. The pressure correction factor F_{PR} and the parameter "n_2" are given by related equations. For water, these parameters are given by eq. (13) and (14) respectively.

$$F_{PR} = 1.733P_r^{0.27} + \left(6.1 + \frac{0.68}{1-P_r}\right)P_r^2 \quad (13)$$

$$n_2 = 0.9 - 0.3P_r^{0.15} \quad (14)$$

2.3 Suppression Factor

The suppression factor S exists in front of the boiling HTC of eq. (1) must be calculated too. Chen [6] was the pioneer of introducing this suppression factor. Then this model was modified by Butterworth [21] and was presented as eq. (15).

$$S_{Chen} = \frac{1}{1 + 2.53\times10^{-6}(Re)^{1.17}} \quad (15)$$

Another suppression factor which introduced by Steiner [12] is the Boiling Departure Lift off, BDL suppression factor. The BDL model attempts to model the flow-induced suppression based on the local dynamics of a vapor bubble subject to the surrounding flow field near the heated surface. Thereby, the BDL model utilizes a concept which was originally proposed by Zeng et al [23]. According to the theory of Zeng, the whole process of vapor bubble lifting-off basically evolves in three different steps as it shown in figure 2. At the first stage the bubble is attached to its nucleation site, and it is inclined by the angle θ<90, due to the hydrodynamic flow forces. The attached bubble is growing until it reaches a critical departure volume V_D where the bubble is dragged of its nucleation site. At this point the volume equivalent departure radius is defined as eq. (16):

$$r_D = \left(\frac{3V_D}{4\pi}\right)^{1/3} \quad (16)$$

In the second stage, θ=0, and the bubbles grow to a point where buoyancy force is enough to lift-off the bubble. Then third stage begins as the bubbles lift-off start. The lift-off radius corresponding to the volume at this stage is as follows:

$$r_L = \left(\frac{3V_L}{4\pi}\right)^{1/3} \quad (17)$$

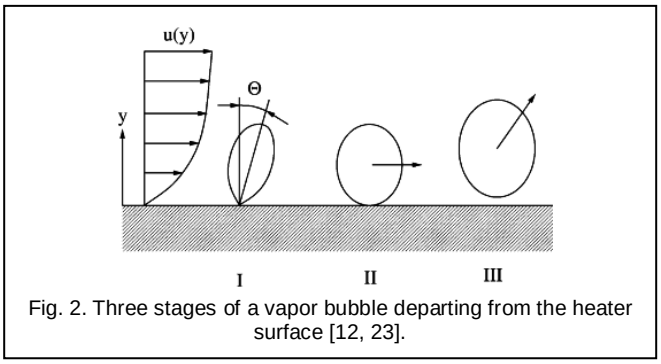

Fig. 2. Three stages of a vapor bubble departing from the heater surface [12, 23].

Based on the above explanation, the flow induced suppression factor is given by eq. (18) [12].

$$S_{flow} = \frac{r_D}{r_L} \quad (18)$$

In the BDL model, the effect of subcooling is also considered and given by eq. (19) [12].

$$S_{sub} = \frac{T_w - T_s}{T_w - T_b} \quad (19)$$

Therefore the total BDL suppression factor is the product of the flow-induced and the subcooling ones.

$$S_{BDL} = S_{flow}\times S_{sub} \quad (20)$$

To obtain the r_D and r_L of the eq. (18) the momentum balance equations along the x and y axis should be solved. As shown in figure 3, the x and y momentum balances are given in eq. (21) and eq. (22) respectively.

$$F_d + F_{du}\sin\theta = 0 \quad (21)$$

$$F_{bcy} + F_{du}\cos\theta + F_{sl} = 0 \quad (22)$$

In the above equations the F_d, F_{du}, F_{bcy} and F_{sl} are drag force, bubble growth force, buoyancy force and shear lift force respectively. The expressions of these forces are given in the eq. (23) to eq. (26) respectively. The effect of surface tension is assumed to be negligible.

$$F_d = 6\mu_l u_r\left\{\frac{2}{3} + \left[\left(\frac{12}{Re_b}\right)^{n_3} + 0.796^{n_3}\right]^{\frac{-1}{n_3}}\right\}, \quad n_3 = 0.65 \quad (23)$$

$$F_{sl} = \frac{3.877}{2}\rho_l u_r^2\pi r_b^2 G_s^{1/2}\left(\frac{1}{Re_b^2} + 0.014G_s^2\right)^{1/4} \quad (24)$$

$$F_{bcy} = \frac{4}{3}\pi r_s^3 \rho_l g \qquad (25)$$

$$F_{du} = \rho_l \pi r_l^2 \left(\frac{3}{2} r_s \dot{r}^2\right) \qquad (26)$$

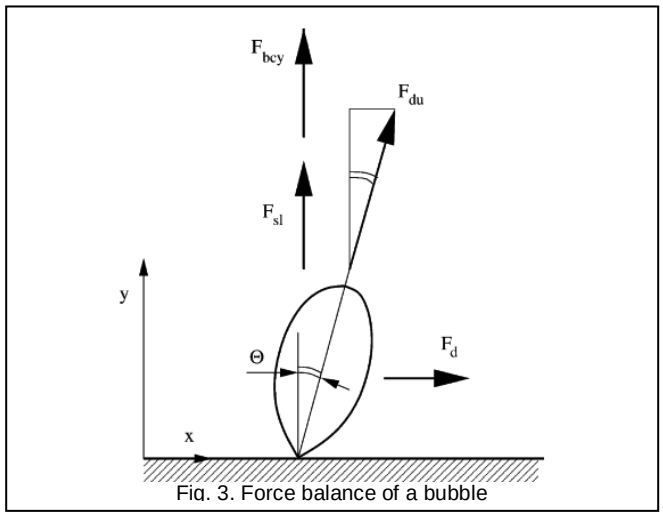

Fig. 3. Force balance of a bubble

In eq. (24), Re_b (is called bubble Reynolds number) and G_s are given as follows.

$$Re_b = \frac{2\rho_l u r}{\mu_l} \qquad (27)$$

$$G_s = \left|\frac{d_u}{d_y}\right|_{y=r} \frac{r}{u} \qquad (28)$$

In the bubble Reynolds number, "u" is the velocity of the flow at the center of the bubble within boundary layer. The C_s imbedded in eq. (26), bubble growth force correlation, is suggested to be 6.67 by [12]. In this equation the radius of the bubble is obtained by eq. (29) presented by Zuber [24].

$$r(t) = \frac{2b}{\sqrt{\pi}} Ja \sqrt{\alpha_l t} \qquad (29)$$

Where the Jacobe number is defined by eq. (30)

$$Ja = \frac{\rho_l C_{p,l}\left(T_w - T_s\right)}{\rho_g h_{lg}} \qquad (30)$$

Parameter "b" is an empirical constant where has been suggested 1.73 for vertical flow [25] and 0.21 for horizontal flow [12].

The velocity profile exists in the momentum equation must be determined first before solving them. Turbulent velocity profile inside the boundary layer can be found from eq. (31).

$$u^+ = y^+ \qquad y^+ \le 5 \qquad (31\text{-a})$$

$$u^+ = 5\ln y^+ - 3.05 \qquad 5 < y^+ < 30 \qquad (31\text{-b})$$

$$u^+ = 2.5\ln y^+ - 5.5 \qquad y^+ \ge 5 \qquad (31\text{-c})$$

Where the y^+ and u^+ are defined by:

$$u^+ \equiv \frac{u_b}{u_\tau^*} = \frac{u_b}{\sqrt{\tau_w/\rho_l}} \qquad (32)$$

$$y^+ \equiv \frac{y u^*}{\nu_l} = \frac{y\sqrt{\tau_w/\rho_l}}{\nu_l} \qquad (33)$$

The wall shear stress can be determined using eq. (34).

$$\tau_w = \frac{1}{2} C_f \rho_l u_l^2 \qquad (34)$$

C_f is the friction coefficient and is defined by

$$C_f = \frac{f}{4} \qquad (35)$$

In order to determine the r_D and r_L, eq. (21) and eq. (22) must be solved at the instant of departure and lift off respectively. Affirmation values must be used in those equations.

At the lift off condition there isn't any slip in the velocity between the bubble and its surrounding liquid. Therefore the drag and shear-lift force and also the inclination angle, θ are zero. Hence for obtaining r_L, the momentum equations reduce to one eq. (36).

$$F_{du} + F_{bcy} = 0 \qquad (36)$$

Eq. (21) and eq. (22) must be solved simultaneously to obtain rD.

As it is shown in figure 4, the accuracy of obtained Sflow which is the ratio of the r_D to r_L, is compared to Steiner et al [12]. Small difference between two diagrams may be related to the usage of different velocity profiles.

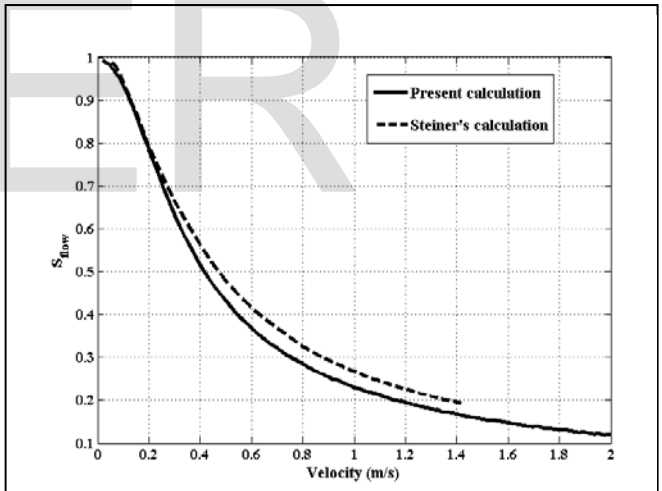

Fig. 4. Comparison of the obtained Sflow in this paper and the Steiner's one

By determining the above parameters, the flow boiling heat flux can be calculated from eq. (37). Four different h_{nb}, i.e. $h_{Rohsenow}$, $h_{Forster\text{-}Zuber}$, h_{Cooper} and $h_{Gorenflo}$ and two suppression factors, S_{Chen} and S_{BDL} are examined in this equation to introduce a new model with higher accuracy.

$$q''_{fb} = h_{fc,Gnielinski}\left(T_w - T_b\right) + h_{nb}\left(T_w - T_s\right) \times S \qquad (37)$$

All these 8 combinations (four nucleate boiling HTC and two suppression factor) results are compared with two different experimental works which are conducted by Robinson [10] and Lee [14]. Finally the best one is chosen and validated with experimental data by present work.

3 EXPERIMENTAL SETUP

3.1 Description

To validate the new proposed correlation an experimental study was conducted thoroughly. In this experiment the flow boiling behavior of both fluids of pure water and mixture of 50-50 water and ethylene glycol was investigated. The Schematic of experimental setup is shown in figure 5. The experimental apparatus is composed of a rectangular duct, test section, heater, variable pump, a reservoir, pre heater, condenser, flow meter, three pressure transducers, aluminum head, copper body, and few thermocouples. The test section (circular surface) with diameter of 15mm is located at the bottom of the rectangular channel and heated by heater as shown in figure 6.

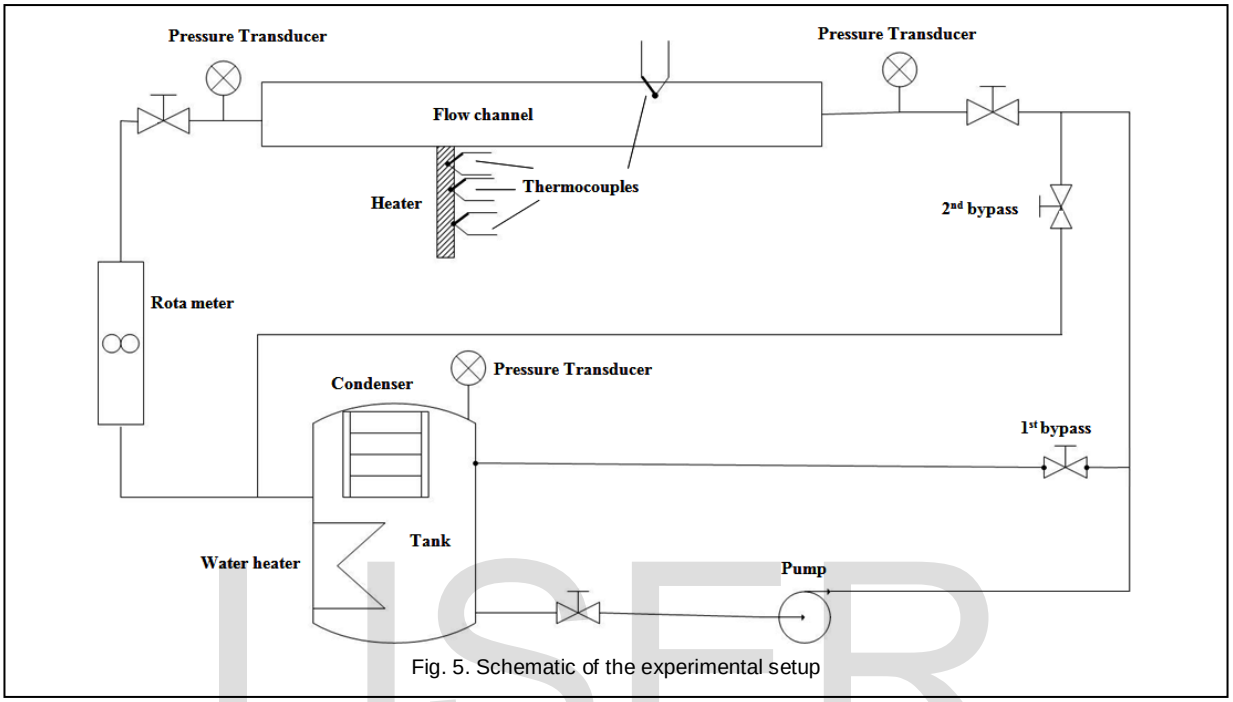

Fig. 5. Schematic of the experimental setup

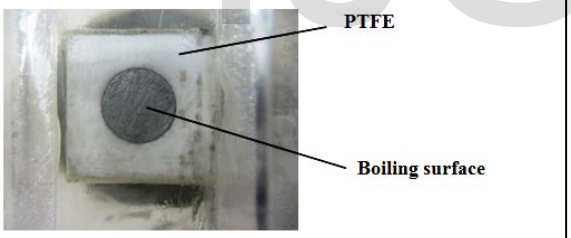

Fig. 4. Test section at the bottom of the channel

This test section is placed 90 cm from inlet of the duct to ensure the flow is hydrodynamically fully developed at this section. The test section surface temperature is evaluated by extrapolating of three measured temperatures along the tip of the test section as shown in figure 7. The aluminum head is mounted on the top of a copper body which is heated by a 1000W rod heater as shown in figure 7. To minimize the heat loss between the aluminum head and the copper body, special high conductivity oil is used at the conjunction. The copper body and aluminum head are well insulated during the test. K-type thermocouples with accuracy of 0.1 K are used in this experiment. To visualize the flow and bubbles, the channel was fabricated with plexy glass panels. Length of the channel is 140 cm and its cross section area is 2×3 cm². To provide the most resemblance to the engine water jacket, the fluid pressure and temperature around the test section was set to be 1.4 bar and 85°C respectively. A pre-heater with a controller was used to control the inlet temperature of the fluid in the reservoir. The pre heater was turned on and off by an on-off controller with respect to the temperature of the fluid in the reservoir. A condenser was used in the reservoir to provide constant pressure and also to condense any existing vapor. All Thermocouples and heater were connected to a data acquisition system (model: ADAM 5000/TCP) to record the experimental data. The flow rate was controlled by two bypass valves and measured by a rotameter (model: GEC- Elliotte) with accuracy of 0.1 L/min. This rotameter is calibrated for pure water at a definite temperature and it must be recalibrated for different fluids with different densities. The following equation is used to calculate the flow rate for different fluids:

$$Q_2 = Q_1\sqrt{\frac{\rho_1(\rho_f - \rho_2)}{\rho_2(\rho_f - \rho_1)}} \tag{38}$$

Where Q_2 and Q_1 are the volumetric flow rate of new fluid and reference one

All the setup was calibrated prior to the data collection. Each test was run few times to make insure its repeatability and their average values were used in each case.

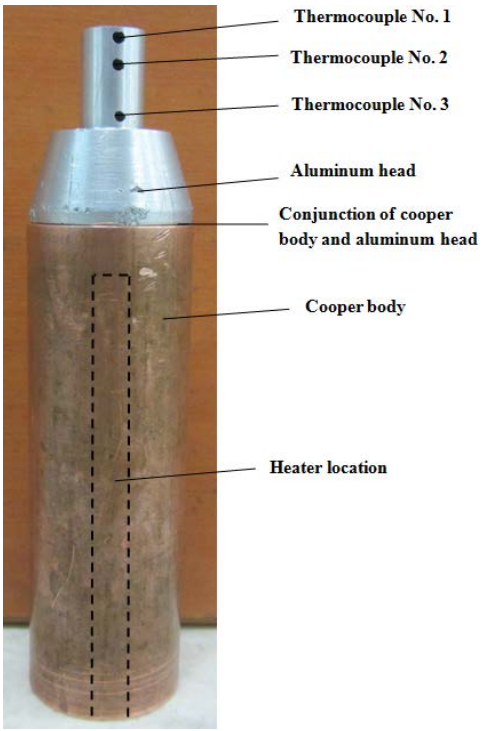

Fig. 7. Cooper body and aluminum head

3.2 Error analysis

In this section the uncertainty of the results is calculated. According to theory of error distribution by Taylor series, equation 38 is used to calculate the uncertainty of a multivariable parameter with 95% certainty [26].

$$U_{95} = \left[\sum_{i=1}^{J} \left(\frac{\partial r}{\partial X_i}\right)^2 U_i^2\right]^{\frac{1}{2}} \quad (39)$$

In this equation U_{95} is the total error of a multivariable parameter r, X_i is an independent variable and U_i is its error and J is the number of variables. The accuracy of each measuring parameters are given in Table 1. These values are provided by the manufacturers.

TABLE 1: ACCURACY OF EACH MEASURING PARAMETERS

variable	symbol	Accuracy
distance	U_x	±0.05mm
Temperature	U_T	±0.1°C
Volume flow rate	U_Q	±2%

In this study the error analysis are carried out for the two main measured parameters, namely the heat flux and temperature. The temperature is an independent variable that its error is given in table 1. But the heat flux is a dependent variable which depends to some variables as it shown in equation 3.

$$q'' = -k\frac{\Delta T}{\Delta x} \quad (40)$$

$$\frac{U_{q''}}{q''} = \sqrt{\left(\frac{U_{\Delta T}}{\Delta T}\right)^2 + \left(\frac{U_{\Delta x}}{\Delta x}\right)^2} \quad (41)$$

$$\frac{U_{q''}}{q''} = 2.7\%$$

With respect to the table 1 and measured data for ΔT and Δx the calculation error of the measured heat flux is about 2.7%.

4 RESULTS AND DISCUSSION

In this section the eight possible combination models are compared with two extensive experimental data carried out by Robinson et al [10] and Lee [14]. All the conditions such as temperature, pressure, channel geometry, fluid type, surface roughness, flow rate and etc are simulated for each case. The comparisons are done for pure water and ICE coolant, 50-50 water-ethylene glycol. As shown in the following figures, the experimental data fall within the predicted results for all cases. The main purpose of this examination is to obtain a general empirical equation for flow boiling heat transfer prediction. Figures 8 to 14 and figures 15 to 18 show the results of the present models along with the Lee and Robinson's experimental data for the water and the 50-50 water-ethylene glycol respectively.

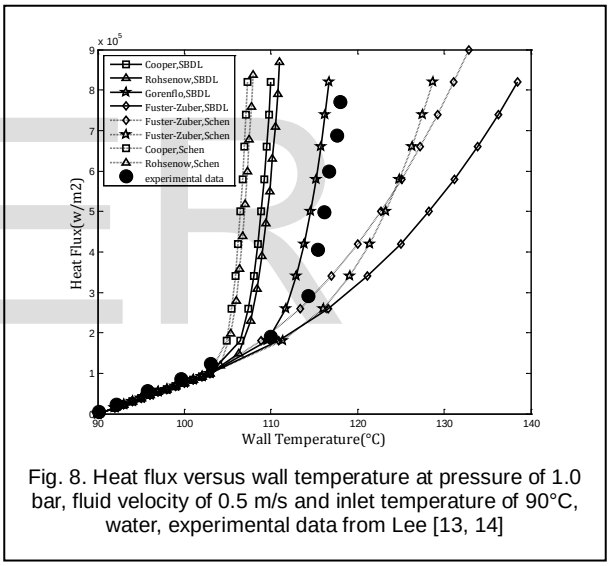

Fig. 8. Heat flux versus wall temperature at pressure of 1.0 bar, fluid velocity of 0.5 m/s and inlet temperature of 90°C, water, experimental data from Lee [13, 14]

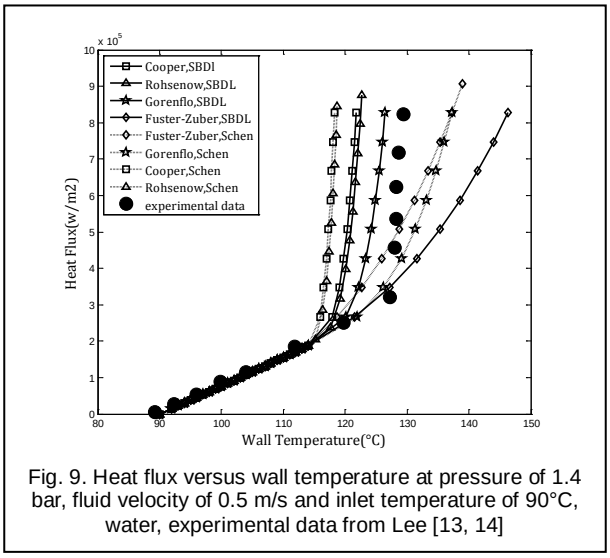

Fig. 9. Heat flux versus wall temperature at pressure of 1.4 bar, fluid velocity of 0.5 m/s and inlet temperature of 90°C, water, experimental data from Lee [13, 14]

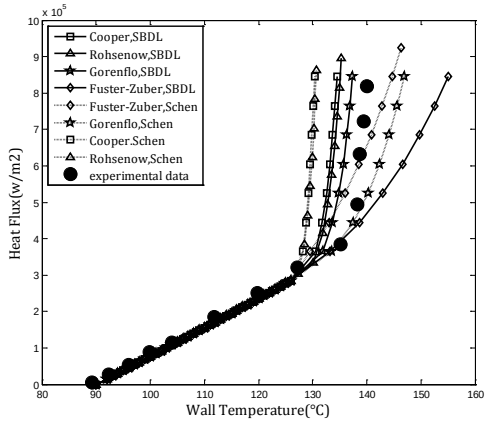

Fig. 10. Heat flux versus wall temperature at pressure of 2.0 bar, fluid velocity of 0.5 m/s and inlet temperature of 90°C, water, experimental data from Lee [13, 14]

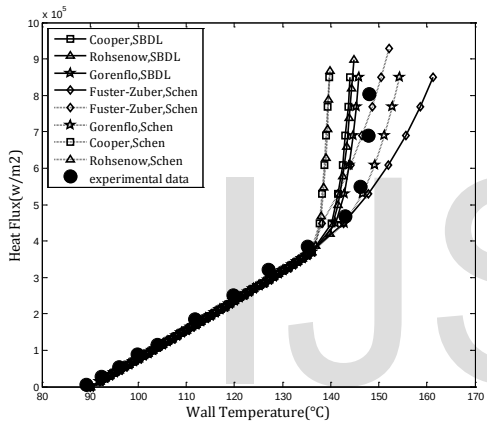

Fig. 11. Heat flux versus wall temperature at pressure of 2.6 bar, fluid velocity of 0.5 m/s and inlet temperature of 90°C, water, experimental data from Lee [13, 14]

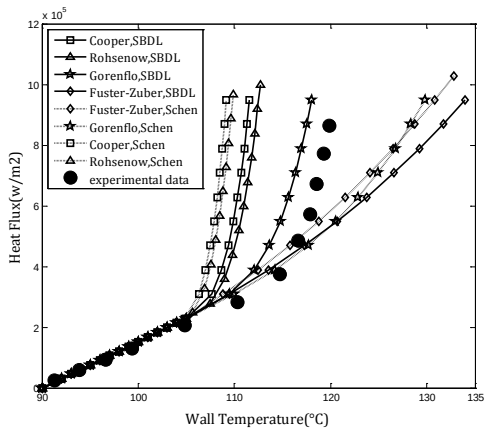

Fig. 12. Heat flux versus wall temperature at pressure of 2.6 bar, fluid velocity of 0.25 m/s and inlet temperature of 90°C, water, experimental data from Lee [13, 14]

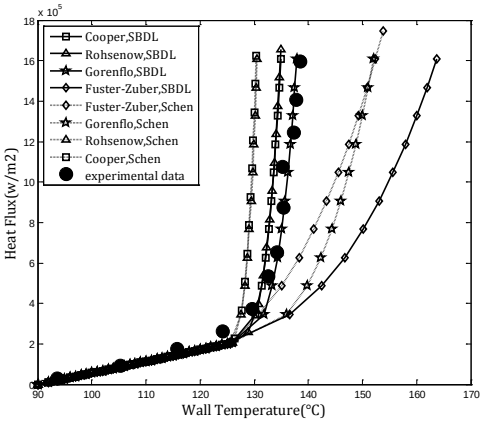

Fig. 13. Heat flux versus wall temperature at pressure of 2.0 bar, fluid velocity of 0.25 m/s and inlet temperature of 90°C, water, experimental data from Robinson [10, 11]

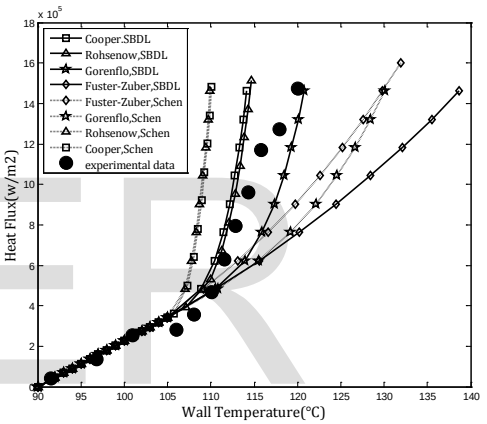

Fig. 14. Heat flux versus wall temperature at pressure of 1.0 bar, fluid velocity of 1.0 m/s and inlet temperature of 90°C, water, experimental data from Robinson [10, 11]

For water it can be observed clearly that the model with $h_{Goren-flo}$ and S_{BDL} gives the more accurate results than the others. Tables 2 and 3 give the average and the maximum error of this case respectively.

TABLE 2: PERCENT OF AVERAGE ERROR OF THE MODEL WITH $H_{GORENFLO}$ AND S_{BDL} FOR WATER AT 90°C

	0.25 m/s	**0.5 m/s**	**1 m/s**
1 bar	2.44	2.09	3.6
1.4 bar	NA	3.03	NA
2 bar	1.11	2.06	NA
2.6 bar	NA	1.91	NA

TABLE 3: PERCENT OF MAXIMUM ERROR OF THE MODEL WITH $H_{GORENFLO}$ AND S_{BDL} FOR WATER AT 90°C

	0.25 m/s	**0.5 m/s**	**1 m/s**
1 bar	2.91	4.23	4.82

1.4 bar	NA	6.3	NA
2 bar	2.22	2.08	NA
2.6 bar	NA	2.18	NA

As it was mentioned earlier, figures 15 to 18 show the results of different flow boiling models for 50-50 water-EG.
For 50-50 water-EG as a coolant of the engine, the flow boiling model with both $h_{Gorenflo}$ and h_{Cooper} along with S_{BDL} shows a good consistency with the experimental data. Tables 4 and 5 give the average and the maximum error of these two models for 50-50 water-EG respectively.

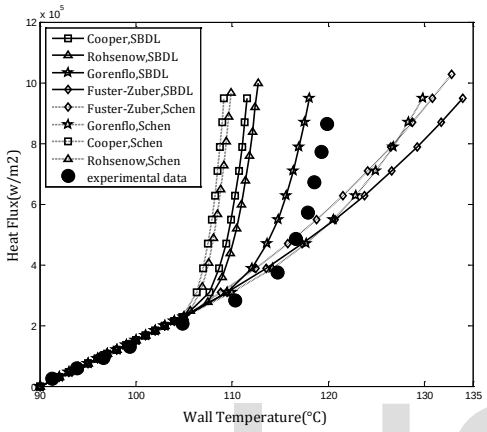

Fig. 15. Heat flux versus wall temperature at pressure of 2.0 bar, fluid velocity of 0.25 m/s and inlet temperature of 90°C, 50-50 water-EG, experimental data from Robinson [10, 11]

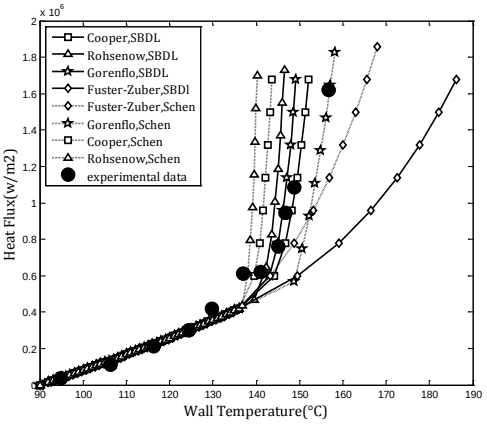

Fig. 16. Heat flux versus wall temperature at pressure of 2.0bar, fluid velocity of 0.5m/s and inlet temperature of 90°C, 50-50 water-EG, experimental data from Robinson [10, 11]

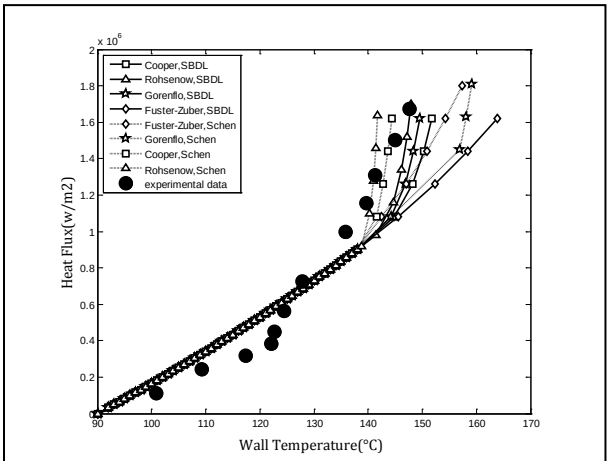

Fig. 17. Heat flux versus wall temperature at pressure of 2.0bar, fluid velocity of 1.0m/s and inlet temperature of 90°C, 50-50 water-EG, experimental data from Robinson [10, 11]

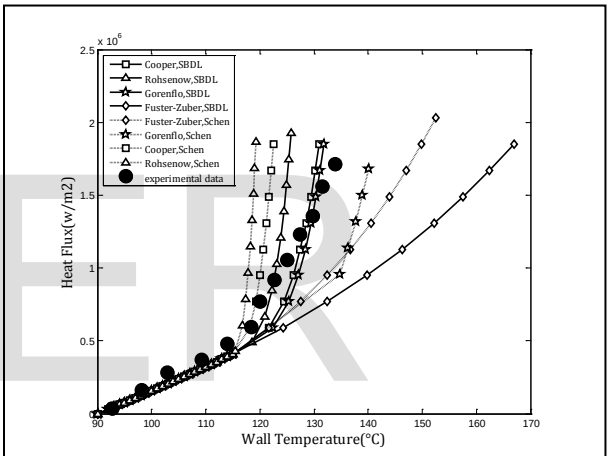

Fig. 18. Heat flux versus wall temperature at pressure of 1.0bar, fluid velocity of 1.5m/s and inlet temperature of 90°C, 50-50 water-EG, experimental data from Robinson [10, 11]

TABLE 4: PERCENT OF AVERAGE ERROR OF THE MODEL WITH $H_{GORENFLO}$ AND H_{COOPER} ALONG WITH S_{BDL} FOR 50-50 WATER-EG AT 90°C

	0.25 m/s		***0.5 m/s***		***1 m/s***		***1.5 m/s***	
	$h_{Gorenflo}$	h_{Cooper}	$h_{Gorenflo}$	h_{Cooper}	$h_{Gorenflo}$	h_{Cooper}	$h_{Gorenflo}$	h_{Cooper}
1	NA	NA	NA	NA	NA	NA	1.78	1.56
2	4.65	4.08	4.57	3.21	3.21	4.05	NA	NA

TABLE 5: PERCENT OF MAXIMUM ERROR OF THE MODEL WITH $H_{GORENFLO}$ AND H_{COOPER} ALONG WITH S_{BDL} FOR 50-50 WATER-EG AT 90°C

	0.25 m/s		***0.5 m/s***		***1 m/s***		***1.5 m/s***	
	$h_{Gorenflo}$	h_{Cooper}	$h_{Gorenflo}$	h_{Cooper}	$h_{Gorenflo}$	h_{Cooper}	$h_{Gorenflo}$	h_{Cooper}
1	NA	NA	NA	NA	NA	NA	3.21	2.94
2	7.63	6.29	6.58	3.21	4.61	5.1	NA	NA

Following these discussion one can conclude that the new obtained model along with $h_{Gorenflo}$ and S_{BDL} predicts more robust and accurate results for both the water and the 50-50 water-EG fluids. In other words the trend of this model follows the experimental data more precisely than the three other models as shown in the figures. It seems there are two reasons to explain why the S_{BDL} predicts better than S_{Chen}. First the bubble-liquid surface impact on the boiling flow is taken into account as explained in [12]. Secondly the surface roughness which influences the velocity field of the flow boiling is considered in this model [12].

It should be noted that the model is closer to the experimental data in the case of water than the mixture of water-EG. This is due to the some constants used in the empirical correlation. The values of these constants are well developed for some fluids such as water and refrigerant [4]. Whereas for others general estimated values are used. Therefore the general estimated values are used for the ICE coolant to predict the flow boiling of the mixture.

The results obtained from the new empirical model were also compared with the collected experimental data to confirm the accuracy of it. Figures 20 to 22 show the comparison for water and figures 23 and 24 for water-EG at different velocities.

As it is seen from figures 19 to 23 the proposed model trend follows the experimental data with good consistency The average error for water velocities of 0.5, 0.75 and 1 m/s are 2.14, 1.34 and 1.39 percent respectively while for the mixture 50-50 water-EG the error in velocities of 0.5 and 0.75 m/s are 2.15 and 3.5 percent. It implies that in the case of 50-50 water-EG, the model has lower accuracy in comparison of water. The lower accuracy of the model for the mixture water-EG can be related to the lack of existing values for the constants used in the empirical equation as mentioned before.

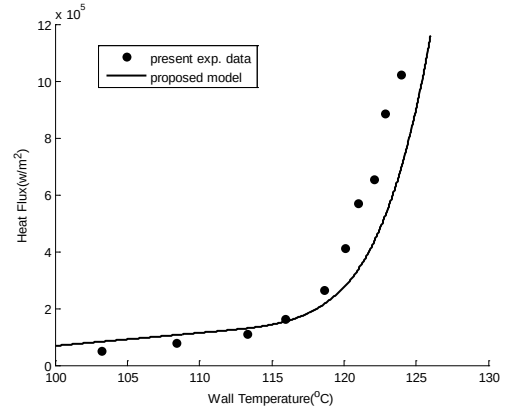

Fig. 19. Heat flux versus wall temperature at pressure of 1.4 bar, fluid velocity of 0.5 m/s and inlet temperature of 85°C, water

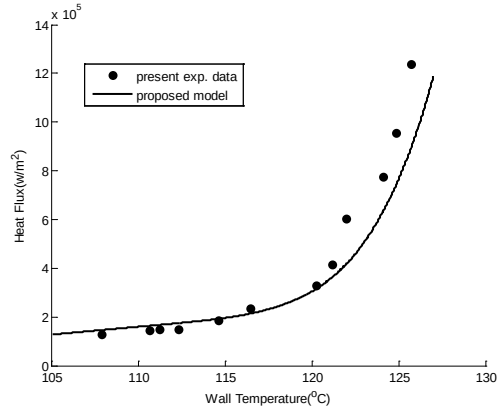

Fig. 20. Heat flux versus wall temperature at pressure of 1.4 bar, fluid velocity of 0.75 m/s and inlet temperature of 85°C, water

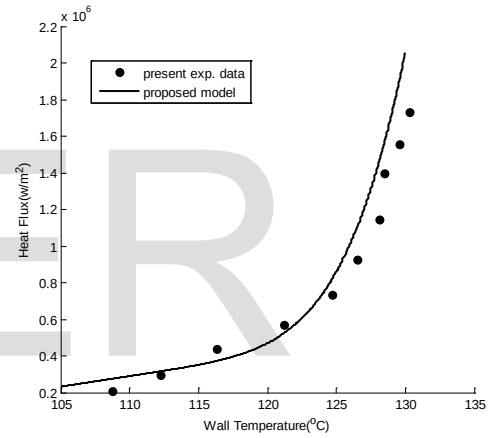

Fig. 21. Heat flux versus wall temperature at pressure of 1.4 bar, fluid velocity of 1 m/s and inlet temperature of 85°C, water

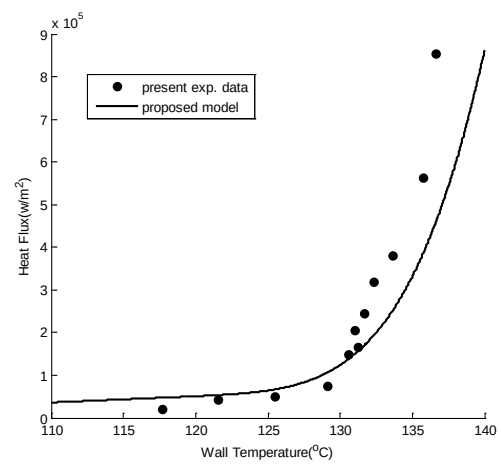

Fig. 22. Heat flux versus wall temperature at pressure of 1.4 bar, fluid velocity of 0.5 m/s and inlet temperature of 85°C, 50-50 water-EG

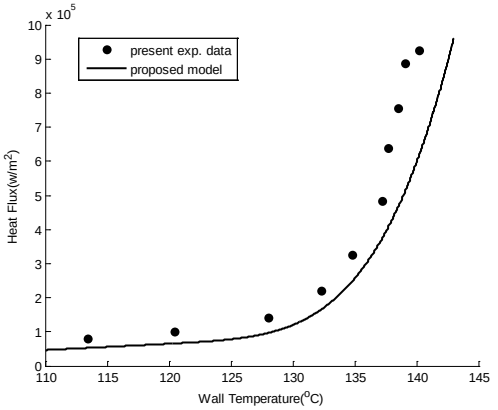

Fig. 23. Heat flux versus wall temperature at pressure of 1.4bar, fluid velocity of 0.75m/s and inlet temperature of 85°C, 50-50 water-EG

5 Conclusion

In this paper the accuracy of different existing models for predicting the internal flow boiling were examined mathematically and experimentally. In general, the flow boiling model consists of two parts, namely force convection and pool boiling. The later one is modified by a parameter called suppression factor. The Gnielinski correlation is used for the force convection term and four different pool boiling models along with two different suppression factors are used to develop a new model. The simulation of the flow boiling for pure water and 50-50 water-ethylene glycol mixtures is carried over a range velocity, 0.25< V <1.5m/s, pressure 1.0< P <2.6bar and the bulk temperature of 90 °C and 85°C respectively. Based on these analyses a new robust and accurate model was developed. The pool boiling heat transfer coefficient, $h_{Gorenflo}$ and BDL suppression factor are used in this model. This new model is then validated with the in house collected experimental data which shows good agreement. The maximum average error predicted with this model for water is 2.14% and for mixture is 3.5%.

References

[1] J.B. Heywood, *Internal Combustion Engine Fundamentals*, Mc GrawHill, Singapore, 1988

[2] M.J. Clough, "Precision Cooling of a Four Valve per Cylinder Engine", SAE 931123

[3] T.L. Bergman, A.S. Lavine, F.P. Incropera, D.P. DeWitt, *Fundamentals of Heat and Mass Transfer*, 7th ed, John Wiley & Sons, USA, 2011

[4] S.M. Ghiaasiaan, *Two phase Flow, Boiling, and Condensation in Conventional and Miniature System*, Cambridge University press, New York, 2008

[5] C. Finlay, and G.R. Gallacher, "The Application of Precision Cooling to the Cylinder Heated of a Small Automotive Petrol Engine", SAE 880263, 1988

[6] C. Chen, "A Correlation for Boiling Heat Transfer to Saturated Fluids in Convective Flow", Ind &Engng Chem - Process Des And Dev 5: 322-329, 1966

[7] F. Dittus, and L. Boelter, "Heat Transfer for Automobile Radiators of the Tubular Type", Univ. of Calif. Publ Engng, 1930

[8] H.K. Forster, N. Zuber, " Growth of a Vapor Bubble in a Superheated Liquid", J Appl Phys 25: 474-478, 1954

[9] N.A.F. Campbell , J.G. Hawley, M.J. Leathard, "Nucleate Boiling Investigation and the Effect of Surface Roughness", SAE 1999-01-0577, 1999

[10] K. Robinson , J.G. Hawly , N.A.F. Campbell , "Experimental and Modeling Aspects of Flow Boiling Heat Transfer for Application to Internal Combustion Engines" Proceedings of the institution of Mechanical Engineers, Part D: Journal of Automobile Engineering, 217-877, 2003

[11] K. Robinson "IC Engine Coolant Heat Transfer Studies" PhD dissertation, University of Bath, UK, 2001

[12] K.H. Steiner, A. Kobor, L. Gebhard, "A Wall Heat Transfer Model for Subcooled Boiling Flow", Int J Heat Mass Transf 48: 4161-4173, 2005

[13] H.S. Lee, A.T. O'Neill , "Comparison of Boiling Curves between a Standard SI Engine and a Flow Loop for a Mixture of Ethylene Glycol and Water", SAE 2006-01-1231, 2006

[14] H.S. Lee, "Heat Transfer Predictions Using the Chen Correlation on Subcooled Flow Boiling in a Standard Engine",. SAE 2009-01-1530, 2009

[15] W.M. Rohsenow, "Heat Transfer with Evaporation", Heat Transfer—A Symposium held at the University of Michigan, 101-150, 1952

[16] I.H. Shames, *Mechanical of fluids*, 4th ed, McGraw Hill, New York, 2002

[17] W.M. Kays, M.E. Crawford ME, *Convective Heat and Mass Transfer*, 3rd ed, McGraw Hill, New York, 1993

[18] W.M. Rohsenow, "A Method of Correlating Heat Transfer Data for Surface Boiling of Liquids", Trans ASME 74:969-975, 1952

[19] W.M. Rohsenow, *Handbook of Heat Transfer*, McGraw Hill, New York, 1973

[20] M.G. Cooper, "Saturation and Nucleate Pool Boiling"—A Simple Correlation. Inst Chem Eng Symp 86: 785, 1984

[21] J.R. Thome, A. Bejan, and A.D. Kraus, *Heat Transfer Handbook*, Wiley, New York, 2003

[22] D. Gorenflo, U. Chandra, S. Kotthoff, A. Luke, "Influence of thermophysical properties on pool boiling heat transfer of refrigerants",. International journal of refrigeration 27: 492-502, 2004

[23] L. Zeng, J. Klausner, D. Bernhard, R. Mei, "A unified model for the prediction of bubble detachment diameters in boiling systems—II Flow boiling", International journal of heat and mass transfer 36: 2271-2279, 1993

[24] N. Zuber, "The Dynamics of Vapour Bubbles in Nonuniform Temperature Fields", Int J Heat Mass Transfer 2: 83-98, 1961

[25] R. Situ, "Bubble Lift-off Size in Forced Convective Subcooled Boiling Flow", Int J Heat and Mass Transfer 48: 5536-5548, 2005

[26] H.W. Coleman, W.G. Steele, *Experimentation and uncertainty analysis for engineers*, Wiley, NewYork, 2009